PHYSICAL REVIEW A **96**, 041804(R) (2017)

Curved-space topological phases in photonic lattices

Eran Lustig,[1] Moshe-Ishay Cohen,[1] Rivka Bekenstein,[1,2,3] Gal Harari,[1] Miguel A. Bandres,[1] and Mordechai Segev[1]
[1]*Physics Department, Technion–Israel Institute of Technology, Haifa 32000, Israel*
[2]*Physics Department, Harvard University, Cambridge, Massachusetts 02138, USA*
[3]*ITAMP, Harvard-Smithsonian Center for Astrophysics, Cambridge, Massachusetts 02138, USA*
(Received 5 July 2017; published 26 October 2017)

We introduce topological phases in curved-space photonic lattices. In such systems, the interplay between the curvature of space and the topology of the system, as manifested in the topology of the band structure, gives rise to a wealth of new phenomena. We demonstrate the topological curved-space concepts in an experimentally realizable setting of a waveguiding layer covering the surface of a three-dimensional body, and show that the curvature of space can induce topological edge states, topological phase transitions, Thouless pumping, and localization effects. We also describe the analogy between our system and topological phases in dynamical curved space-time settings known from general relativity.

DOI: 10.1103/PhysRevA.96.041804

Topological insulators constitute a growing field of research in condensed matter [1–4] as well as in other fields of science. They are particularly interesting since they support transport that is protected against disorder due to the material's topological nature. Extending the topological ideas beyond condensed matter started with the prediction of topological phenomena with electromagnetic waves [5,6] and experiments with microwaves in gyro-optic media [7]. Research on topological phenomena in photonics began with the experiments on topological edge states in a binary lattice [8] and on Thouless pumping in quasiperiodic lattices [9]. The next stage was the search for photonic topological insulators [10–12], that have topologically protected unidirectional transport of photons. Photonic topological insulators were demonstrated in 2013 in two different systems [13,14]. Since then, topological photonics has been flourishing with many new ideas [15–18] and conceptual applications for devices based on topology [10,19,20]. More recently, topological phenomena have also been observed with cold atoms [21,22], acoustic waves [23,24], and mechanical waves [25]. Interestingly, recent pioneering work has demonstrated a photonic system emulating a two-dimensional (2D) gas on a cone with Landau levels [26], which is essentially a curved-space setting [27,28]. Clearly, exploring topological phases in curved-space systems, known from general relativity (GR), can add new fundamental features to the area of topological physics. Moreover, although experiments involving gravitational space-time curvature are rarely accessible in the laboratory [29], it is possible to construct systems realizing curved-space settings in optics [30–44], Bose-Einstein condensates [45–47], and acoustics [48–50], providing platforms for demonstrating GR phenomena [47], triggering new insights.

Here, we present topological phases in curved-space photonic lattices. We study lattices in the presence of a curved spatial metric, specifically in cases where the topological phases are determined by the metric. Our study is carried out in the context of photonics, but the concepts involved are universal, having manifestations in many areas of physics. We study the effects in an experimentally viable physical setting, a thin 2D waveguiding layer covering the surface of a three-dimensional (3D) body [51–53], where the light effectively propagates in 2D curved space. We show that, by engineering the curvature of the surface (analogous to changing the spatial metric underlying the photonic propagation), we induce topological phases, topological phase transitions, Thouless pumping, and localization effects.

Consider a laser beam propagating in a thin waveguiding layer covering the surface area of a curved 3D body [51,52], as sketched in Fig. 1(a). For simplicity, the surface is azimuthally symmetric about the Cartesian axis z. This surface of revolution (SOR) is described by the 2×2 metric g given by $ds^2 = r(z)^2 d\theta^2 + dz^2 = R(z)^2 dx^2 + dz^2 = g_{xx}(z)dx^2 + g_{zz}dz^2$, where $r(z)$ is the polar radius, θ is the azimuthal angle, $dx = r(z=0)d\theta$ is the azimuthal angle scaled to units of length, $R(z)$ is dimensionless, and g_{zz}, g_{xx} are the diagonal components of g that depend only on z. For such 2D SORs, the polar radius $r(z)$ is used as a means to control the curvature of space.

We are interested in photonic topological phenomena that result from the curved metric of space. Since many topological systems rely on periodic potentials, we introduce a lattice structure to the metric, $g_{xx}(z) = \sum_n f(z - z_n)$, where $f(z)$ describes a locally confined contraction or expansion of space, and z_n are the locations of these local distortions of space. This means that space is contracting in a repeating form [Fig. 1(a)]. Lattices based on metric curvature were demonstrated experimentally in photonic systems [54]. Here, we construct the metric component g_{xx} to have the structure of a lattice with a topologically nontrivial band structure, and show that topological edge states can appear and disappear depending on the curvature of space.

Consider surfaces with a small intrinsic and extrinsic curvature [with $r(z)$ large compared to the optical wavelength, such as the hollow cylinder sketched in Fig. 1(a)], of radius $r(z)$ and thickness h, with a periodic lattice fabricated on it. Here, the azimuthal symmetry of the surface allows the decoupling of Maxwell's equations [51–53] according to $\psi(x,z,h) = \phi(x,z)\Xi(h)$, where ψ is a linearly polarized electric field. Under these assumptions (see the Supplemental Material [55]), a coherent beam propagating paraxially in the x direction [normal to the axis of revolution z; Fig. 1(a)], obeys

$$2ik_x \frac{\partial u(x,z)}{\partial x} = -\frac{g_{xx}(z)}{g_{zz}} \frac{\partial^2 u(x,z)}{\partial z^2} - V_{\text{eff}} u(x,z), \qquad (1)$$

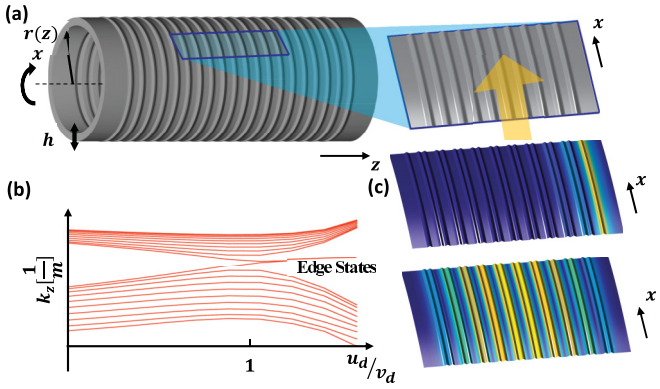

FIG. 1. (a) A cylindrical waveguiding layer with an imprinted curved SSH lattice. The yellow arrow indicates the direction of light propagation. (b) Energy spectrum of the curved-space SSH as a function of the ratio of distances u_d/v_d; both u_d and v_d depend only on the metric. (c) Eigenmodes of the curved space SSH lattice. The color map represents the light intensity: Light propagating in a topological edge mode (upper) and in a nontopological mode when the system is topologically trivial (lower).

where $\phi(x,z) = g_{zz}^{1/4} g_{xx}^{-1/4} u(x,z) \exp[ik_x x]$, $V_{\text{eff}} = -\frac{3}{16 g_{zz}} \frac{(g'_{xx})^2}{g_{xx}^2} + \frac{1}{4 g_{zz}} \frac{g''_{xx}}{g_{xx}}$, and k_x is the (approximate) propagation constant (x component of the wave number). Equation (1) is analogous to the one-dimensional (1D) Schrödinger equation, where x plays the role of time. The space metric $g(z)$ introduces two important effects: First, it creates an effective potential that depends on the derivatives of the curvature. Second, and more importantly, it makes the "mass" term [first term on the right-hand side of Eq. (1)] dependent on the local curvature. Since Eq. (1) is effectively a linear 1D Schrödinger equation, its eigenvectors and eigenvalues can be calculated numerically.

Next, we describe how light can propagate in topological edge states that form strictly due to the space curvature. We examine the Su-Schrieffer-Heeger (SSH) binary lattice model [56,57], which is the simplest model exhibiting topologically protected edge states [58]. The SSH has two coupling constants u and v, and two phases: topological, when the lattice ends on a site with the smaller coupling constant and an edge state exists, and trivial, when the lattice ends on a site with the larger coupling constant and no edge state exists. The topological invariant characterizing each phase is found by integrating the Zak phase of the infinite bulk over the Brillouin zone [58,59]. Although the SSH model is relatively simple, it has a topological phase that is related directly to the edge states of 2D systems such as graphene ribbons [60]. To construct an analog to the SSH model in curved space, we use the scheme depicted in Fig. 1(a), with $g_{xx}(z) = G_0 + \sum_n G(z - z_n)$, where n is the site index,

$$z_n - z_{n-1} = \begin{cases} u_d, & n \text{ even}, \\ v_d, & n \text{ odd}, \end{cases}$$

u_d and v_d are distances between neighboring sites, G_0 is a constant basic curvature of the surface, and

$$\mathrm{G(z)} = \begin{cases} A\left[1 + \cos\left(\frac{z}{\mathrm{w}}\right)\right], & -\pi < \frac{z}{\mathrm{w}} < \pi, \\ 0, & \text{else}, \end{cases}$$

where A and w are fixed amplitude and width [61]. The structure has small enough derivatives ($|\partial_z g_{xx}| \ll |q g_{xx}|$) such that V_{eff} is negligible [62]. We compute the eigenenergies of Eq. (1), and find that this curved-space setting indeed supports topological edge states and a continuum of bulk states [Figs. 1(b) and 1(c)]. Specifically in Fig. 1(b), the horizontal axis (along which a topological phase transition occurs) is completely determined by the curvature. This shows how the curvature of space, alone, can support a topological phase in a real physical system.

Next, we examine the effects of a temporally varying space curvature on lattices with topological phases. Some of the most interesting GR phenomena arise when the space curvature is time dependent. As with many GR effects, it is very challenging to measure these effects, but one can find analogous systems for which a coordinate plays the role of time and the curvature depends on that coordinate. Indeed, having dynamics in time plays a major role in topological systems, because systems that are driven by some external time-dependent force can exhibit a topological phase transition [63,64]. Here, we find that if a lattice has a space curvature that varies in time, it is possible to observe topological phase transitions driven solely by changing the metric in time. We will now show a scheme where the light is propagating in the z direction on a SOR, with the curvature changing as a function of the "time coordinate" z. By tailoring these curvature variations we can cause dramatic effects on a lattice with topological phases. We now describe a SSH lattice in which the uniform contraction or expansion of space can cause topological phase transitions, and explain how this is different from the flat-space SSH lattice.

Consider paraxial propagation in the z direction on a SOR, similar to Ref. [51], and add a small perturbative potential $\Delta n(x,z)$ (which satisfies: $|2k_0^2 n_0 \Delta n(x,z)| \ll k_0^2 n_0^2$) in the form of a lattice potential [array of waveguides, Figs. 2(a) and 2(b)]. Then, using the paraxial approximation and the ansatz $\phi(z,x) = \frac{1}{g_{xx}^{1/4}} u(z,x) e^{iqz} e^{-i/2q \int_0^{z'} V_{\text{eff}}(z')dz'}$, where $V_{\text{eff}}(z) = \frac{1}{16}\left[\frac{3}{g^2} g'^2_{xx} - \frac{1}{4 g_{xx}} g''_{xx}\right]$, we obtain the Schrödinger-like equation for light propagating in a curved-space setting with a lattice potential,

$$i \frac{\partial}{\partial z} u(z,x) = -\frac{1}{2q g_{xx}(z)} \frac{\partial^2}{\partial x^2} u(z,x) - \frac{k_0^2 \Delta n(z,x)}{n_0 q} u(z,x). \tag{2}$$

This equation is analogous to the 1D Schrödinger equation, where z plays the role of time, and the space metric $g(z)$ is causing the expansion or compression of the x axis (scaled by the azimuthal angle). The two terms on the right-hand side of Eq. (2) represent the kinetic energy and the lattice potential. Note that Eqs. (1) and (2), although seemingly similar, represent two very different cases: Equation (1) represents propagation perpendicular to the symmetry axis of the SOR,

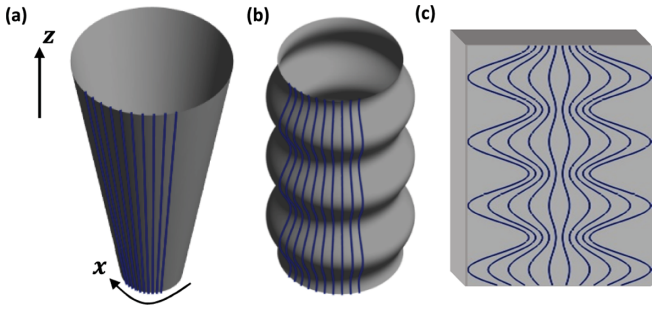

FIG. 2. Lattices in dynamical curved space. (a), (b) Lattices of evanescently coupled waveguides (blue) on a light guiding cone (a) and on a periodic sinusoidal surface of revolution (b). (c) The flat-space potential obtained from (b) after mapping it to a flat plane, keeping the relative distances between waveguides the same (the outer waveguides in the lattice go through a longer optical path and stronger oscillations in amplitude than the waveguides in the middle of the lattice).

while Eq. (2) describes evolution in the direction parallel to the symmetry axis of the SOR.

Let us first explain the basic difference between a curved-space lattice and a similar lattice in flat space. The propagation of light in a curved-space lattice can be treated, to first order in curvature, as a system in flat space subjected to artificial gauge fields. For example, for the SOR system, transforming the x coordinate in Eq. (2) to the "flat" coordinate $x' = \sqrt{g_{xx}}x$, neglecting high orders of $g_{xx}'(z)$ and using $u' = u(x,z)e^{-\frac{1}{2}\int \frac{[\sqrt{g_{xx}(z)}]_z}{\sqrt{g_{xx}(z)}}dz}$ (that changes only the amplitude as a function of z, but since z plays the role of time it can be renormalized for every z), gives

$$i\frac{\partial}{\partial z}u'(z,x') = -\frac{1}{2q}\left(\frac{\partial}{\partial x'} + iq\frac{[\sqrt{g_{xx}(z)}]_z}{\sqrt{g_{xx}(z)}}x'\right)^2 u'(z,x') - \frac{k_0^2\Delta n(z,x')}{n_0 q}u'(z,x'). \quad (3)$$

When neglecting high orders of $g_{xx}'(z)$, Eq. (3) is equivalent to Eq. (2). However, the effect of the curvature appears in Eq. (3) as a gauge field instead of as a mass term [Eq. (2)]. This mapping means that, to first order of the curvature derivative, a lattice in curved space is equivalent to the same lattice in flat space [Figs. 2(b) and 2(c)] but subjected to an additional metric-dependent gauge field that is linear in x'. The consequence of this gauge field is that phase accumulation in z for all the waveguides is the same, under a uniform compression or expansion of space. For example, contracting the transverse coordinate x as the coordinate z is increasing means shortening the separation between waveguides. This, in a 2D flat space, results in that the light in different waveguides accumulates different phases as it evolves in z. In contrast, in a SOR all accumulated phases are the same for all the waveguides, when shortening the separation between waveguides. Thus, waveguiding on a SOR is different than in flat space, in a fundamental way (beyond just affecting the distance between waveguides), and this is reflected in this gauge field, which acts as an effective electric field in Eq. (3). Also, if we compare Fig. 2(b) to Fig. 2(c) in the first-order analysis, the outer waveguides of the lattice depicted in Fig. 2(c) radiate much more (at a rate increasing with the size of the lattice) than the outer waveguides of the lattice in Fig. 2(b), due to the structure of the SOR.

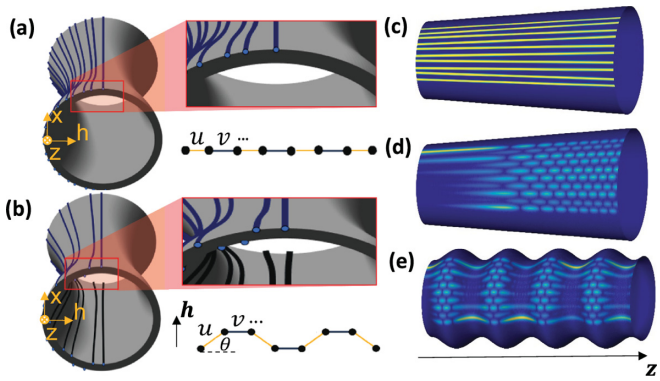

FIG. 3. Topological phase transition induced by the curvature of space. (a) SSH lattice with a topological phase which is invariant to the expansion of space in x. The blue lines are waveguides embedded in the guiding SOR. (b) SSH lattice with a topological phase that depends on the expansion of space in x. The waveguides are placed in the inner and the outer side of the shell. If $u\sin\theta < v$, the uniaxial expansion induces a topological phase transition. (c) Realization of a SSH lattice on a SOR that is effectively the lattice of (b) on a small segment (in z) near the phase transformation. When Δz is small, the separation between waveguides changes approximately linearly with z. The yellow lines are the potential wells and the blue surface is the SOR. (d) Adiabatic propagation of light in the potential of (c) during a phase transition from topological (edge states exist) to trivial (no edge states). (e) Adiabatic propagation in an oscillatory SOR. The light alternates between bulk states and edge states as the topological phase changes due to periodic changes in the metric.

Next, we show how to induce a topological phase transition by uniformly shrinking the space that underlies the SSH lattice. The SSH lattice on a SOR is plotted in Fig. 3(a). Changing the radius of the surface, which is equivalent to a uniform expansion of space in the x direction, does not change the topological phase of the SSH lattice, since the ratio u/v remains constant. However, it is possible to design a SSH lattice that does not preserve the ratio of the coupling coefficients even under uniaxial expansion, as illustrated in Figs. 3(b) and 3(c). Such a lattice enables relating the uniform expansion of space in the x direction to the topological phase of the lattice. This can be realized by a cylindrical dielectric shell whose thickness is small compared to its radius $h \ll R$. For such SSH lattices, the ratio u/v changes upon changing the radius of the shell [Fig. 3(c)]. If $u\sin\theta < v$ for the angle θ plotted in Fig. 3(b), then a topological phase transition can occur upon expansion or contraction of the SOR. This condition ($u\sin\theta < v$) divides these lattices into two classes. One class, for which $u\sin\theta > v$, has nontrivial topology that preserves the topological phase for any expansion or contraction (and any θ). The other class, for which $u\sin\theta < v$, has trivial topology that does not conserve the topological phase upon expansion or contraction.

The propagation of light in a SSH lattice in curved space that expands (e.g., an expanding cone) exhibits a topological phase transition [Fig. 3(d)]. In all waveguides the light is

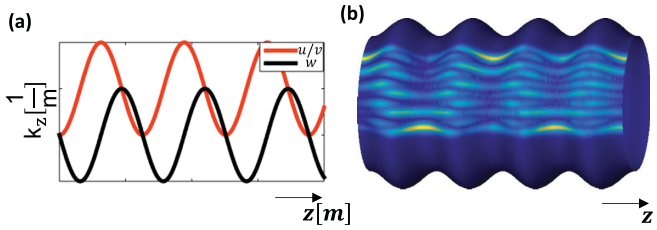

FIG. 4. Thouless pumping induced by curved space. (a) The coupling coefficients ratio u/v (red line) and the staggered potential w (black line) in the lossy Rice-Mele pump as a function of z. (b) Propagation in an oscillating sinusoidal SOR with a staggered potential obtained by changing the width of the waveguides as a function of curvature according to the black line in (a). Most of the power is pumped from one side to the other periodically, with the same period as the curvature variation.

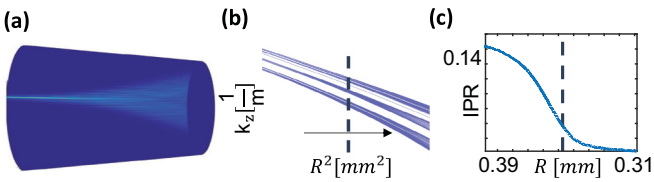

FIG. 5. (a) Delocalization in a contracting Andre-Aubry-Harper lattice (AAH). Propagation in an AAH lattice on a cone, going from the region $t < p$, where all the modes are localized, to the $t > p$ region, where all the modes are extended. Light injected into a single waveguide remains localized until the duality point at $t = p$, after which the beam expands. (b) Energy spectrum of the AAH lattice as a function of the radius of the SOR. The arrow signifies that the cone crosses the duality point marked by the dashed line. (c) Inverse participation ratio of the model in (a) as a function of the radius.

accumulating phase at the same rate [Eq. (3)], such that the light remains in the initial state during a contraction that preserves small $g'_{xx}(z)$. The geometry of the SOR preserves translational symmetry under contraction, unlike contraction in a flat plane for which the lattice experiences an effective gauge (electric) field that destroys the translational symmetry. Since translational symmetry is preserved in a SOR, along with all other symmetries of the SSH, the curved-space SSH experiences a topological phase transition. In such a phase transition, the localized edge state transforms adiabatically into a bulk state, which is an extended state [65]. Of course, the evolution of the curvature of space does not have to be monotonic: It can be periodic or even random, as long as it evolves adiabatically in Eq. (2), so as to ensure that the states transform adiabatically with negligible couplings between the different modes of the system. For example, Fig. 3(e) shows the adiabatic propagation in the lattice of Fig. 2(b) on a periodic curved SOR with $g_{xx}(z) = [1 + \sin(\Omega_\gamma z)]^2$. As shown in Fig. 3(e), the light bounces between the bulk and the edges periodically, due to a topological phase transition that occurs periodically and adiabatically. This relation between metric variations and topological invariants enables also to control at which edge the light will be, i.e., trigger Thouless pumping of power from one edge to the other. The pumping (Fig. 4) is done by making the on-site energy of the waveguides dependent on the metric, according to the Rice-Mele scheme [Fig. 4(a)] [66]. The rate in at which the pumping occurs is the metric's period of oscillations. The pumping results in the transfer of power from one edge to the other at exactly the same periodicity as the metric [Fig. 4(b)].

Finally, we demonstrate how the dynamics of the metric can change drastically the behavior of light in a system exhibiting a band structure with nontrivial topology. In what we show next, varying the curvature of space nonadiabatically in a quasidisordered lattice with a topological band structure breaks the localization of light in the system [65]. For this purpose, we use the Andre-Aubry-Harper (AAH) model [67], which is a quasiperiodic lattice described by

$$H\psi_n = t(\psi_{n+1} + \psi_{n-1}) + 2p\cos(2\pi bn + \phi)\psi_n, \qquad (4)$$

where ψ_n is the amplitude at site n, t is the hopping coefficient, and p is the on-site energy coefficient. Setting b to be irrational makes the lattice quasiperiodic. This model has edge states (when truncated), and displays a topological band structure, and a duality point at $t = p$ [67]. The duality results from the fact that Fourier transforming Eq. (4) with $\phi = 0$ does not change its functional form, only causing t and p to switch places. Thus, since the differences in on-site energies localize all the states when $t < p$, the duality implies that when $t > p$, all the states are localized in Fourier space, hence they are extended states in real space.

Consider a truncated lattice with waveguides that are equally spaced on a cone (except the edges) and have on-site energies (tuned by controlling the width of the waveguides) according to the AAH model [Eq. (4)]. The curvature changes

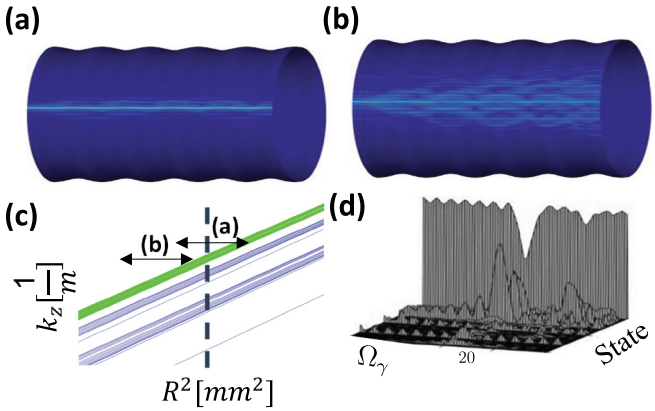

FIG. 6. Dynamic curvature-induced delocalization in an AAH lattice. (a) Propagation of an eigenstate in the AAH lattice under oscillating curvature in the $t < p$ regime. The light remains localized and behaves as if the system is adiabatic. (b) The same frequency and amplitude of the metric as in (a) but with average radius around the $t = p$ point. The light delocalizes in a nonadiabatic way. (c) Part of the energy spectrum as a function of the SOR radius; the arrows signify the oscillations of the models (a) and (b), the dashed line is the duality point, and only the green band's states couple in the settings of (a) and (b). (d) Projection of the beam at z_{final} on the eigenstates of the system (vertical axis) for each eigenstate (horizontal axis), after propagation in an oscillating SOR in the localized regime ($t < p$), for various frequencies Ω_γ (second horizontal axis). There is a resonance at the metric frequency $\Omega_\gamma = 20[\frac{1}{m}]$.

the ratio between t and p. Starting with Eq. (2) and some algebra, it is possible to show that the AAH model maintains its functional form [Eq. (4)] for small changes in g, by using a tight-binding approach. This setting enables one to explore the dynamics of the system around the duality point. When the SOR is wide ($t < p$), all states are localized. In contrast, when the SOR is narrow ($t > p$), all the states are extended states. The transition during propagation [Figs. 5(a)–5(c)] occurs at $t = p$ and it is adiabatic if the contraction and expansion are slow enough [65]. To quantify how localized or extended the propagating wave is, we use the inverse participation ratio, defined by $\sum_i |\psi|^2 / \sum_i |\psi|^4$ [68], where i goes over the lattice sites and ψ is the propagating field [Fig. 5(c)].

Placing the AAH lattice on the sinusoidal curved SOR of Fig. 2(b) allows one to study the effects of curved-space dynamics on the propagation, and its connection to the topological band structure. The oscillations of space (at frequency Ω_γ) couple two states A and B if Ω_γ matches their k_z difference ($k_{z,A} - k_{z,B} \approx \Omega_\gamma$) and if they have a nonzero spatial overlap integral. This gives rise to unique delocalization effects within the AAH model due to the curvature of space. When the radius of the SOR does not cross the duality point ($t = p$) during the oscillations [Fig. 6(a)], the states behave as if the oscillations are "adiabatic," and do not couple to any other state, staying localized. However, when the SOR begins to cross the duality point [Fig. 6(b)] while keeping the frequency of oscillations constant, the system behaves in a "nonadiabatic" way and an initially localized state delocalizes more and more in every cycle, until light spreads over the entire lattice, thus exhibiting a "nonadiabatic" behavior. This behavior can be explained in the following way: The evolving state can only couple within a certain band (in the topological band structure) since in our case Ω_γ is smaller than the gap in k_z [Fig. 6(c)]. But when $t < p$, the states in that band are not close to each other spatially, so their overlap integral is negligible. On the other hand, when the oscillations go through $t = p$, the overlap integral grows rapidly and all the states in the band couple to each other, so the states delocalize and stay delocalized even when the radius widens again, corresponding to $t < p$. The only way the states can delocalize, when $t < p$ during the entire propagation, is through resonances between different bands [Fig. 6(d)].

To conclude this Rapid Communication about topological phases in curved-space lattices, we note that these ideas can be implemented in experiments, with light propagating in lattices imprinted on a thin waveguiding layer covering a 3D body, as the structures fabricated by the NanoScribe in Ref. [69]. The analysis can be extended to nonlinear effects where the intensity affects the topological phenomena directly.

ACKNOWLEDGMENTS

This work was supported by the Israel Science Ministry, by the US Air Force Office for Scientific Research, by the Israel Science Foundation, and by the German-Israeli DIP Project.

[1] C. L. Kane and E. J. Mele, Phys. Rev. Lett. **95**, 146802 (2005).
[2] B. A Bernevig and S.-C. Zhang, Phys. Rev. Lett. **96**, 106802 (2006).
[3] M. König, S. Wiedmann, C. Bröne, A. Roth, H. Buhmann, L. W. Molenkamp, X.-L. Qi, and S.-C. Zhang, Science **318**, 766 (2007).
[4] D. Hsieh, D. Qian, L. Wray, Y. Xia, Y. S. Hor, R. J. Cava, and M. Z. Hasan, Nature (London) **452**, 970 (2008).
[5] Z. Wang, Y. D. Chong, J. D. Joannopoulos, and M. Soljačić, Phys. Rev. Lett. **100**, 013905 (2008).
[6] S. Raghu and F. D. M. Haldane, Phys. Rev. A **78**, 033834 (2008).
[7] Z. Wang, Y. Chong, J. D. Joannopoulos, and M. Soljačić, Nature (London) **461**, 772 (2009).
[8] N. Malkova, I. Hromada, X. Wang, G. Bryant, and Z. Chen, Opt. Lett. **34**, 1633 (2009).
[9] Y. E. Kraus, Y. Lahini, Z. Ringel, M. Verbin, and O. Zilberberg, Phys. Rev. Lett. **109**, 106402 (2012).
[10] M. Hafezi, E. A. Demler, M. D. Lukin, and J. M. Taylor, Nat. Phys. **7**, 907 (2011).
[11] R. O. Umucalılar and I. Carusotto, Phys. Rev. A **84**, 043804 (2011).
[12] A. B. Khanikaev, S. H. Mousavi, W.-K. Tse, M. Kargarian, A. H. MacDonald, and G. Shvets, Nat. Mater. **12**, 233 (2013).
[13] M. C. Rechtsman, J. M. Zeuner, Y. Plotnik, Y. Lumer, D. Podolsky, F. Dreisow, S. Nolte, M. Segev, and A. Szameit, Nature (London) **496**, 196 (2013).
[14] M. Hafezi, S. Mittal, J. Fan, A. Migdall, and J. M. Taylor, Nat. Photonics **7**, 1001 (2013).
[15] Y. Lumer, Y. Plotnik, M. C. Rechtsman, and M. Segev, Phys. Rev. Lett. **111**, 243905 (2013).
[16] M. A. Bandres, M. C. Rechtsman, and M. Segev, Phys. Rev. X **6**, 011016 (2016).
[17] S. Mittal, S. Ganeshan, J. Fan, A. Vaezi, and M. Hafezi, Nat. Photonics **10**, 180 (2016).
[18] L. J. Maczewsky, J. M. Zeuner, S. Nolte, and A. Szameit, Nat. Commun. **8**, 13756 (2017).
[19] M. C. Rechtsman, Y. Lumer, Y. Plotnik, A. Perez-Leija, A. Szameit, and M. Segev, Optica **3**, 925 (2016).
[20] G. Harari, M. A. Bandres, Y. Lumer, Y. Plotnik, D. N. Christodoulides, and M. Segev, Topological lasers, in *Conference on Lasers and Electro-Optics*, OSA Technical Digest (online) (Optical Society of America, Washington, D.C., 2016), paper FM3A.3.
[21] G. Jotzu, M. Messer, R. Desbuquois, M. Lebrat, T. Uehlinger, D. Greif, and T. Esslinger, Nature (London) **515**, 237 (2014).
[22] M. Aidelsburger, M. Lohse, C. Schweizer, M. Atala, J. T. Barreiro, S. Nascimbène, N. R. Cooper, I. Bloch, and N. Goldman, Nat. Phys. **11**, 162 (2015).
[23] A. B. Khanikaev, R. Fleury, S. H. Mousavi, and A. Alù, Nat. Commun. **6**, 8260 (2015).
[24] C. He, X. Ni, H. Ge, X.-C. Sun, Y.-B. Chen, M.-H. Lu, X.-P. Liu, and Y.-F Chen, Nat. Phys. **12**, 1124 (2016).
[25] R. Süsstrunk and S. D. Huber, Science **349**, 47 (2015).
[26] N. Schine, A. Ryou, A. Gromov, A. Sommer, and J. Simon, Nature (London) **534**, 671 (2016).
[27] X. G. Wen and A. Zee, Phys. Rev. Lett. **69**, 953 (1992).

[28] J. E. Avron, R. Seiler, and P. G. Zograf, Phys. Rev. Lett. **75**, 697 (1995).
[29] B. P. Abbott *et al.*, Phys. Rev. Lett. **116**, 061102 (2016).
[30] U. Leonhardt and P. Piwnicki, Phys. Rev. A **60**, 4301 (1999).
[31] U. Leonhardt and P. Piwnicki, Phys. Rev. Lett. **84**, 822 (2000).
[32] I. I. Smolyaninov, New J. Phys. **5**, 147 (2003).
[33] T. G. Philbin, C. Kuklewicz, S. Robertson, S. Hill, F. König, and U. Leonhardt, Science **319**, 1367 (2008).
[34] E. E. Narimanov and A. V. Kildishev, Appl. Phys. Lett. **95**, 041106 (2009).
[35] D. A. Genov, S. Zhang, and X. Zhang, Nat. Phys. **5**, 687 (2009).
[36] F. Belgiorno, S. L. Cacciatori, M. Clerici, V. Gorini, G. Ortenzi, L. Rizzi, E. Rubino, V. G. Sala, and D. Faccio, Phys. Rev. Lett. **105**, 203901 (2010).
[37] A. Demircan, Sh. Amiranashvili, and G. Steinmeyer, Phys. Rev. Lett. **106**, 163901 (2011).
[38] C. Sheng, H. Liu, Y. Wang, S. N. Zhu, and D. A. Genov, Nat. Photonics **7**, 902 (2013).
[39] S. Batz and U. Peschel, Phys. Rev. A **81**, 053806 (2010).
[40] I. I. Smolyaninov, Phys. Rev. A **88**, 033843 (2013).
[41] E. Karen, M. Erkintalo, Y. Xu, N. G. R. Broderick, J. M. Dudley, G. Genty, and S. G. Murdoch, Nat. Commun. **5**, 4969 (2014).
[42] S. F. Wang, A. Mussot, M. Conforti, A. Bendahmane, X. L. Zeng, and A. Kudlinski, Phys. Rev. A **92**, 023837 (2015).
[43] R. Bekenstein, R. Schley, M. Mutzafi, C. Rotschild, and M. Segev, Nat. Phys. **11**, 872 (2015).
[44] C. Sheng, R. Bekenstein, H. Liu, S. Zhu, and M. Segev, Nat. Commun. **7**, 10747 (2016).
[45] C. Barceló, S. Liberati, and M. Visser, Phys. Rev. A **68**, 053613 (2003).
[46] P. O. Fedichev and U. R. Fischer, Phys. Rev. Lett. **91**, 240407 (2003).
[47] J. Steinhauer, Nat. Phys. **12**, 959 (2016).
[48] W. G. Unruh, Phys. Rev. Lett. **46**, 1351 (1981).
[49] R. Schützhold and W. G. Unruh, Phys. Rev. D **66**, 044019 (2002).
[50] S. Weinfurtner, E. W. Tedford, M. C. J. Penrice, W. G. Unruh, and G. A. Lawrence, Phys. Rev. Lett. **106**, 021302 (2011).
[51] S. Batz and U. Peschel, Phys. Rev. A **78**, 043821 (2008).
[52] R. Bekenstein, J. Nemirovsky, I. Kaminer, and M. Segev, Phys. Rev. X **4**, 011038 (2014).
[53] V. H. Schultheiss, S. Batz, and U. Peschel, Nat. Photonics **10**, 106 (2016).
[54] Most interestingly, the pioneering work by A. Szameit *et al.* [Phys. Rev. Lett. **104**, 150403 (2010)] has demonstrated, in experiments, the optical analog of a quantum geometric potential. The topology in that setting (topology of the metric) is fundamentally different from the topologies giving rise to topological insulators (topologies of the bands), and therefore does not have topological edge states and topological protection, which are the fundamental cornerstones of the field of topological insulators.
[55] See Supplemental Material at http://link.aps.org/supplemental/10.1103/PhysRevA.96.041804 for a brief description of the derivation..
[56] W. P. Su, J. R. Schrieffer, and A. J. Heeger, Phys. Rev. Lett. **42**, 1698 (1979).
[57] A. J. Heeger, S. Kivelson, J. R. Schrieffer, and W.-P. Su, Rev. Mod. Phys. **60**, 781 (1988).
[58] S. Ryu and Y. Hatsugai, Phys. Rev. Lett. **89**, 077002 (2002).
[59] J. Zak, Phys. Rev. Lett. **62**, 2747 (1989).
[60] P. Delplace, D. Ullmo, and G. Montambaux, Phys. Rev. B **84**, 195452 (2011).
[61] The second derivative of $G(z)$ is discontinuous, and since we work with numerical computations, this is not causing significant problems.
[62] Had V_{eff} not been negligible but dominant, the edge states would be destroyed since V_{eff} by itself is a potential that lacks edge states.
[63] T. Kitagawa, E. Berg, M. Rudner, and E. Demler, Phys. Rev. B **82**, 235114 (2010).
[64] N. H. Lindner, G. Refael, and V. Galitski, Nat. Phys. **7**, 490 (2011).
[65] The adiabaticity here is in the context of the separation of the lattice modes, that is, the variation in the metric due to the curvature is much smaller than the separation among the propagation constants of the modes.
[66] M. J. Rice and E. J. Mele, Phys. Rev. Lett. **49**, 1455 (1982).
[67] S. Aubry and G. André, Ann. Israel Phys. Soc. **3**, 33 (1980).
[68] T. Schwartz, G. Bartal, S. Fishman, and M. Segev, Nature (London) **446**, 52 (2007).
[69] R. Bekenstein, Y. Kabessa, Y. Sharabi, O. Tal, N. Engheta, G. Eisenstein, A. J. Agranat, and M. Segev, Nat. Photonics **11**, 664 (2017).